

Properties of Formation Mechanism of the Hydrothermally-Synthesized ZrW_2O_8

Elena S. Dedova^{1, 2, 3, a)}, Sergei N. Kulkov^{1, 2, 3, b)}, and Fernando Pedrasa^{4, c)}

¹ Institute of Strength Physics and Materials Science SB RAS, Tomsk, 634055, Russia

² National Research Tomsk State University, Tomsk, 634050, Russia

³ National Research Tomsk Polytechnic University, Tomsk, 634050, Russia

⁴ 223, avenue Albert Einstein, La Rochelle, 170071, France

a) Corresponding author: lsdedova@yandex.ru

b) kulkov@ms.tsc.ru

c) vp-ri@univ-lr.fr

Abstract. A single-phase ZrW_2O_8 was prepared using the hydrothermal synthesis by decomposition of $ZrW_2O_7(OH_{1.5}Cl_{0.5}) \cdot 2H_2O$. The formation mechanism of ZrW_2O_8 was described. The morphology of the material was represented as elongated particles with an intrinsic block structure. The stability fields of ZrW_2O_8 were determined. The ZrW_2O_8 demonstrated a negative thermal expansion behavior in the temperature range from 25°C to 750°C. Introduction of ZrW_2O_8 particles as reinforcement element into a metal matrix can lead to the formation of an internal stress caused by the difference between values of thermal expansion of matrix and reinforcing additives, which improve its mechanical properties.

Keywords: zirconium tungstate; hydrothermal synthesis; negative thermal expansion coefficient

INTRODUCTION

The development of new materials that exhibit unusual properties is one of the most rapidly developing areas of modern materials science. There are the materials characterized by negative thermal expansion (NTE) and that contract upon heating. Usually, the contraction is moderate and anisotropic, and it appears in a narrow temperature range only. ZrW_2O_8 is a perspective material due to its isotropic NTE ($\alpha = -9 \times 10^{-6} \text{C}^{-1}$ in the temperatures range from -273°C to 770°C) [1]. Zirconium tungstate can be very useful in the technology of composites. The practical use of the composites containing ZrW_2O_8 implies continuous operation under various conditions, including severe temperatures. On this basis, it is necessary to study the temperature behavior of ZrW_2O_8 . Thermal analysis and *in situ* high-temperature X-ray studies will provide important information on the structural and phase transformations occurring in the process of material heating and reveal the mechanism of hydrothermally-produced ZrW_2O_8 .

MATERIALS AND EXPERIMENTAL PROCEDURE

The following substances were used as source components for the production of a precursor: $Na_2WO_4 \cdot 2H_2O$ (AR grade), $ZrOCl_2 \cdot 8H_2O$ (CP grade) and HCl (CP grade). Aqueous solutions of $Na_2WO_4 \cdot 2H_2O$ (0.5 mol/L), $ZrOCl_2 \cdot 8H_2O$ (0.25 mol/L), HCl (8 mol/L) were thoroughly mixed and placed into a Teflon-lined stainless steel autoclave. The hydrothermal reaction was conducted at 160°C for 36 hours. The product was repeatedly rinsed with distilled water and dried at 110°C. High-temperature *in situ* XRD analyses of the powder were conducted using Bruker D8 diffractometer with CuK_{α} source of filtered radiation at the Boreskov Institute of Catalysis of SB RAS. The analyses of particle form and size were conducted using JEM-2100 transmission electron microscope (TEM) and Phillips SEM 515 scanning electron microscopy (SEM). The commercially pure aluminum (ASD 6) was mixed

with the obtained ZrW_2O_8 powder at various ratios (0.1, 0.5, 1, 5 and 10 wt.%). The powder mixture was compacted and sintered at 600°C for 1 hour. The testing of Vickers hardness was conducted using PMT-3 harness gauge. Axial compression testing was performed using Instron 1185 device with the loading speed of 0.2 mm/s.

RESULTS AND DISCUSSION

Formation Mechanism of ZrW_2O_8

The initial powder of hydrothermally-synthesized $\text{ZrW}_2\text{O}_7(\text{OH},\text{Cl})_2 \cdot 2\text{H}_2\text{O}$ precursor included two kinds of particles: agglomerates consisting of elongated filamentary particles ($\langle d \rangle = 0.6$ nm) and individual elongated particles. The distribution of elongated particles by size (longitudinal and lateral) had a unimodal nature. With increasing temperature from 25°C to 350°C the average longitudinal size of the elongated particles varied from 2 nm to 1 μm . The average lateral size of the elongated particles was 0.2 μm . The calculation showed that the activation energy of particles was 8 kJ/mol in the temperature range from 25°C to 350°C , while in the range from 350°C to 600°C it was equal to 1 kJ/mol (Fig. 1). The abrupt change of the activation energy for the temperature ranging from 200°C to 300°C evidences either the changes in the crystal lattice or the occurrence of a phase transition.

In situ XRD studies were used to investigate the mechanism of ZrW_2O_8 formation. At temperatures under 200°C only $\text{ZrW}_2\text{O}_7(\text{OH},\text{Cl})_2 \cdot 2\text{H}_2\text{O}$ peaks were observed [2]. XRD patterns at the temperature of up to 500°C showed that the entire material went over to X-ray amorphous state. A further increase of the temperature up to 600°C lead to the formation of a crystalline structure that can be identified as cubic zirconium tungstate. The lattice parameter of the resulting cubic modification at 600°C is equal to 9.1211 Å, which agrees well with the literature data (9.1540 Å) [1]. For 700°C along with ZrW_2O_8 diffraction peaks there are those of WO_3 . The further increase of the temperature to 1000°C lead to the decomposition of ZrW_2O_8 into WO_3 and ZrO_2 . Figure 2 demonstrates the dependence of the ratio of integral intensity of all X-ray reflexes to the background intensity ($\Sigma I/I_b$) on the temperature. This dependence was linearly approximated. There is an intersection point at 365°C . The decrease of $\Sigma I/I_b$ down to 400°C witnesses an amorphization and the further increase of the temperature is due to the material crystallization. Probably, the formation of ZrW_2O_8 occurs through the X-ray amorphous phase, which can be interpreted as a meso-nano transformation.

The formation of hydrothermally-synthesized ZrW_2O_8 proceeds in two stages: 1) transition of the crystalline $\text{ZrW}_2\text{O}_7(\text{OH},\text{Cl})_2 \cdot 2\text{H}_2\text{O}$ precursor into the X-ray amorphous state with the activation energy of 8 kJ/mol; 2) nucleation of ZrW_2O_8 at $350 \pm 25^\circ\text{C}$ and the growth of nuclei up to the temperature reaching 550°C ($Q = 1$ kJ/mol).

Properties of ZrW_2O_8

Observations of the morphology of zirconium tungstate using a transmission electron microscopy showed that ZrW_2O_8 powder consisted of elongated particles with an intrinsic block structure.

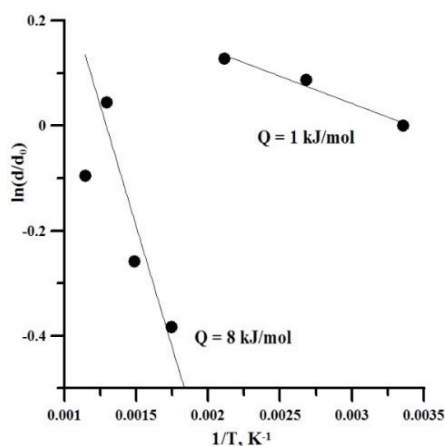


FIGURE 1. Dependence of particle size change of $\text{ZrW}_2\text{O}_7(\text{OH}_{1.5}\text{Cl}_{0.5}) \cdot 2\text{H}_2\text{O}$ on temperature

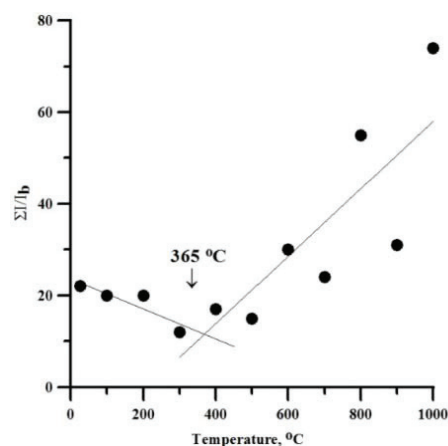


FIGURE 2. Dependence of ratio of total intensity of all X-ray reflexes to background intensity on temperature

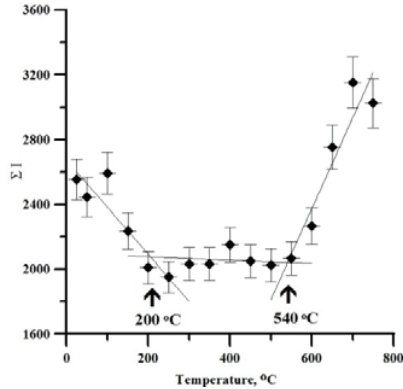


FIGURE 3. Dependence of total intensity (ΣI) of all X-ray reflexes on temperature

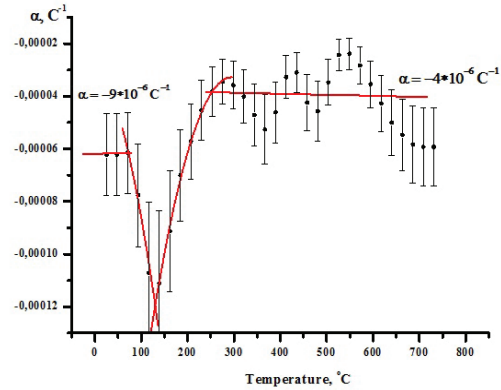


FIGURE 4. Dependence of coefficient of ZrW_2O_8 thermal expansion on temperature

The average block size varied from 20 nm to 50 nm. The average lateral size of the elongated particles varied from 30 nm to 700 nm, and the average longitudinal size varied from 0.5 μm to 5.0 μm . The developed ZrW_2O_8 crystals inherit the shape and the size of $ZrW_2O_7(OH_{1.5}Cl_{0.5}) \cdot 2H_2O$ crystals.

The results of high-temperature *in situ* XRD observations of ZrW_2O_8 showed a gradual decrease of the intensity of reflexes from surfaces (1 1 1), (2 2 1) and (3 1 0) up to the complete disappearance of the said reflexes at the temperatures exceeding 200°C [3]. According to [1], peak disappearance is connected with the transition from a low-temperature α - ZrW_2O_8 ($P2_13$) modification to a high-temperature β - ZrW_2O_8 ($Pa3$) modification, the transition being induced by the increase of a space group symmetry. The increase to 600°C lead to the appearance of weak diffraction lines that correspond to WO_3 and ZrO_2 . A further increase of the temperature up to 750°C lead to the increase of the peak intensity of WO_3 , the appearance of ZrO_2 lines and the decrease of ZrW_2O_8 reflexes.

Figure 3 demonstrates the dependence of the total intensity (ΣI) of all X-ray reflexes on temperature derived from the results of XRD analysis. Below 200°C, the total intensity goes down. Increasing the temperature from 200°C to 540°C lead to the variation of ΣI within the value of experimental uncertainty. The further increase of the temperature up to 750°C resulted in the increase of the total reflex intensity. The intersection points of approximating lines correspond to 200°C and 540°C. According to the X-ray diffraction data, the drop of the total intensity was initiated by the $\alpha \rightarrow \beta$ transition and, as a consequence, by the disappearance of some reflexes. For the temperature below 540°C there is only the high-temperature β - ZrW_2O_8 modification. The increase of the total intensity up to 540°C can be explained by a beginning of the formation of new structures. Atoms in the zirconium tungstate structure begin to rearrange to form sublattices of tungsten and zirconium oxides. Presumably, this movement of atoms precedes the decomposition of zirconium tungstate. It is known [1, 3] that zirconium tungstate loses its kinetic stability and decomposes into ZrO_2 and WO_3 at the temperatures above 770°C. According to XRD analysis, weak lines of WO_3 and ZrO_2 were observed in diffraction patterns at the temperature above 540°C. The coefficient of thermal expansion was equal to $-9.4 \times 10^{-6} C^{-1}$ for α - ZrW_2O_8 and $-3.8 \times 10^{-6} C^{-1}$ for β - ZrW_2O_8 .

Properties of Al- ZrW_2O_8

Materials with anomalous thermal properties may become very useful in various applications of the composites technology. Composites with a negative coefficient of thermal expansion (CTE) may become very useful in various applications: stomatology, thermal protection systems, high precision optical mirrors, fiber optic systems. Moreover, implantation of ZrW_2O_8 particles as reinforcement element into a metal matrix one can obtain the composites with high strength properties. The increase of strength properties is caused by the difference between values of thermal expansion of metal and ZrW_2O_8 . Aluminum is the most easily accessed metal for studying the metal hardening due to its wide application as a construction material. The calculations showed that the internal compression stresses are generated due to the CTE difference and can reach 2 GPa in comparison with Orowan mechanism where $\Delta\sigma \sim 20$ MPa.

The structure and mechanical properties of Al- ZrW_2O_8 containing 0.1, 0.5, 1, 5 and 10 wt.% of zirconium tungstate were studied. The SEM analysis showed that on the polished surface of specimens includes white particles (Fig. 5).

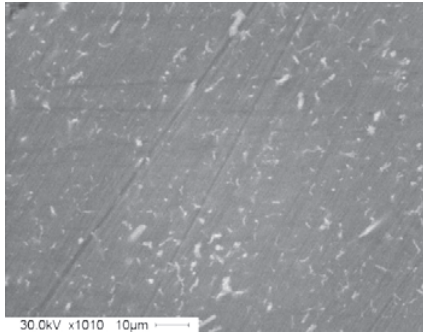


FIGURE 5. SEM pictures of Al with 10 wt.% of ZrW_2O_8

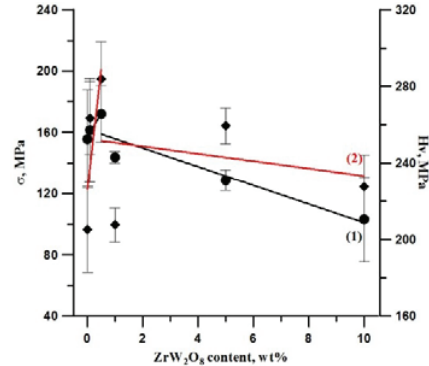


FIGURE 6. Dependence of ultimate compression strength (1) and Vickers hardness on ZrW_2O_8 content (2)

The EDAX analysis showed that these particles contain Zr, W and O atoms, the correlation of the number of atoms being in a good agreement with ZrW_2O_8 stoichiometry ($Zr : W = 1 : 2$). The average grain size of particles significantly increased with the increasing concentration of ZrW_2O_8 and did not exceed $1 \mu m$ for Al with 10 wt.% of ZrW_2O_8 .

From the XRD analysis it was shown that only peaks corresponding to cubic aluminum and cubic zirconium tungstate were observed. The obtained lattice parameters of aluminum and ZrW_2O_8 slightly deviate from the literature, which could be caused by microalloying of the matrix due to either the interaction during sintering process or presence of internal residual compressive stresses in the material. In the second case the compressive stresses in matrix can reach 260 MPa.

Implantation of zirconium tungstate improved the mechanical properties of aluminum. Fig. 7 shows the dependence of the ultimate compression strength and the Vickers hardness of Al- ZrW_2O_8 on the content of zirconium tungstate. The highest values of hardness H_v and strength σ were achieved with the introduction of up to 0.5 wt.% of ZrW_2O_8 and were equal to 284 MPa and 172 MPa, respectively. The further increase of ZrW_2O_8 concentration up to 10 wt.% deteriorates the material mechanical properties.

CONCLUSION

The formation of hydrothermally-synthesized ZrW_2O_8 proceeded in two stages: 1) transition of the crystalline $ZrW_2O_7(OH,Cl)_2 \cdot 2H_2O$ precursor into the X-ray amorphous state with the activation energy of 8 kJ/mol; 2) nucleation of ZrW_2O_8 at $350 \pm 25^\circ C$ and the growth of nuclei up to temperature reaching $550^\circ C$ ($Q = 1$ kJ/mol). It was established that the zirconium tungstate retains its crystal structure in the range of temperatures less than $540^\circ C$. The further increase of temperature is accompanied by the change of ZrW_2O_8 structure induced by the occurrence of WO_3 and ZrO_2 phases, which precedes the decomposition of zirconium tungstate into constituent oxides at the temperatures above $750^\circ C$. The phase transition from the low-temperature (α) to high-temperature (β) modification of cubic zirconium tungstate occurs at $200^\circ C$. The coefficients of thermal expansion of zirconium tungstate powder were: $-9.6 \times 10^{-6} C^{-1}$ for α - ZrW_2O_8 and $-3.8 \times 10^{-6} C^{-1}$ for β - ZrW_2O_8 . It was found that the introduction of 0.5 wt.% of ZrW_2O_8 leads to the increase of mechanical properties of the Al- ZrW_2O_8 ($H_v = 284$ MPa, $\sigma = 172$ MPa) compared with the same properties of pure aluminum.

ACKNOWLEDGEMENTS

This work was partially supported by Agreement No. 14.575.21.0040 (powders sintering part). Authors are grateful to T. Yu. Kardash from Boreskov Institute of Catalysis SB RAS for help in powders sintering (shared use center "NANOTECH").

REFERENCES

1. T. A. Mary, J. S. O. Evans, T. Vogt, and A. W Sleight, *Science* **272**, 90 (1996).
2. S. N. Kulkov, E. S. Dedova, and A. I. Gubanov, *Izv. Vyssh. Uchebn. Zaved. Fiz.* **56**(12/2), 151 (2013).
3. E. S. Dedova, V. S. Shadrin, A. I. Gubanov, and S. N. Kulkov, *Perspekt. Mater.*, 5, 22 (2014).